

Mean First-Passage Time Calculations for the Coil-to-Helix Transition: The Active Helix Ising Model[†]

Nicolae-Viorel Buchete and John E. Straub*

Department of Chemistry, Boston University, Boston, Massachusetts 02215

Received: January 31, 2001; In Final Form: May 11, 2001

The kinetics and thermodynamics of the coil-to-helix transition is studied using a one-dimensional “Zimm–Bragg” Ising model. The mean first-passage time for the coil-to-helix transition is estimated within the “mean sequence” approximation. A generalized mean first-passage time equation is derived where the transition rates may depend on the state of the system. The analytic expression for the mean first-passage time is evaluated, and the results are discussed as a function of energetic parameters, nucleation and propagation constants, peptide length, and the initial fraction of coil. The equilibrium thermodynamic properties of the model are shown to agree well with the Zimm–Bragg model, validating the mean sequence approximation. The time scales for helix formation are computed for a range of energetic parameters that determine the nucleation and propagation constants for the model. It is shown that, for a range of thermodynamically realistic parameters, the kinetic first-passage times are on the order of those measured experimentally. The mean first-passage time approach implicitly allows for the possibility of multiple helix nucleation sites and multiple helical domains and makes no assumptions regarding the unidirectionality of helix propagation. Comparison is made with the predictions of the “sequential kinetics” model of Brooks and the “kinetic zipper” model of Thompson et al. Extension of the model to the more general case of structure formation in proteins is discussed.

1. Introduction

It is hard to overestimate the importance of the helix-coil transition in the development of the theoretical models concerned with the protein folding problem. The commonality of the helical fold and its physical properties made it one of the first candidates for studying secondary structure formation in polypeptides. The helix-coil transition justly became one of the central topics in many classical biophysics textbooks.^{1,2}

Over the last forty years, many successful models were developed for the *equilibrium* properties of the helix-coil transition. The early thermodynamic treatment of Schellman³ was probably the first successful theoretical model that explained with some accuracy the equilibrium properties of the helix-coil transition. Many experiments employing infrared spectroscopy, optical rotation, or viscosity measurements were used to investigate the transition. Most relied on the theoretical procedure set forth by Schellman to interpret their results by estimating the equilibrium constants for the *nucleation* and *propagation* steps of the transition. This type of theoretical treatment was widely used to develop the very popular *zipper* model which assumes that the helical residues of a given polypeptide chain are contiguous.³ The zipper model is especially useful in analyzing the thermodynamic properties of short peptides as no prior assumption regarding the length of the chain of residues is made.

The more accurate models of Zimm–Bragg (ZB)⁴ and Lifson–Roig⁵, appropriate for long peptides, are based on calculations in which no prior assumption is made as to the length or number of helical segments in the polypeptide. In such models, all possible statistical states with the correct combina-

torial weights are taken into consideration in computing the peptide’s energetics. In particular, the ZB model has become the standard minimal description of the helix-coil equilibrium in terms of “nucleation” (σs) and “propagation” (s) constants. The model is isomorphic with the one-dimensional Ising model for arbitrary spin–spin coupling (J) and external field (H)

$$\mathcal{H} = -J \sum_{\langle ij \rangle} s_i s_j - H \sum_i s_i \quad (1)$$

where J and H are expressed in units of kT . A helical residue is taken to be “spin up” (with spin unity) and a coil residue “spin down” (with spin zero). The relation between the two sets of parameters, as shown in ref 6 is essentially

$$\sigma s = \exp(H) \quad s = \exp(J + H) \quad (2)$$

These relations are introduced as a standard notation in the helix-coil transition literature. The exact values of σs and s depend on the specific model that is considered. We will show that these relations are a good approximation for the model that we are developing for calculating the time scale of the coil-to-helix transition, but we are going to use a more accurate numerical method for estimating the dependency of σs and s on J and H .

The pioneering work of Scheraga and co-workers demonstrated how “host–guest” methods on substituted homopolymeric polypeptides could be used to determine the σ and s parameters for a variety of amino acids.^{1,7} That and similar work demonstrated that the ZB model and its variants could be used to successfully organize and interpret data on equilibrium properties of the helix-coil transition in polypeptides. The ZB model captures the general features of the helix-coil equilibrium, including the dependence of the helicity θ on temperature, helix length (N), and nucleation and propagation constants.

[†] Part of the special issue “Bruce Berne Festschrift”.

* To whom correspondence should be addressed. Phone: (617) 353-6816. Fax: (617) 353-6466. E-mail: straub@bu.edu.

The above-mentioned models were developed for the calculation of equilibrium thermo-statistical averages. They do not address aspects of the dynamics and the time scale of the transition including the exact dependence of the transition time on the *nucleation* and *propagation* equilibrium constants. Although there is general agreement on the features of the equilibrium properties of the coil-to-helix transition, there is no current consensus on the time scale for helix propagation or folding. A variety of experimental studies have provided widely varying estimates. Early experimental estimates of the time scale of helix propagation were taken to be on the order of 1 ns with helix folding occurring on the 1 μ s time scale.⁸ Early molecular dynamics simulations of Daggett and Levitt led to an estimate of the time scale for helix propagation on the order of 100 ps.⁹ Brooks developed a kinetic model parametrized using detailed energetics derived from computer simulations of an alanine polypeptide¹⁰. On the basis of the results, he argued that helix folding could occur on a nanosecond time scale. More recently, laser temperature-jump experiments by Thompson et al. found the helix propagation rate to occur on the time scale of 10 ns.¹¹ Coarse grained molecular dynamics simulations of helix formation found that the helix folding time could vary from 6 ns to 1 μ s; at the folding transition temperature, the time scale was found to be roughly 20 ns.¹² These estimates indicate that the helix propagation occurs on a time scale of 10 ns to 1 μ s. Nevertheless, in a recent study Clarke and co-workers have argued that the time scale for helix folding of a polyalanine based polypeptide occurs on a 1 ms time scale.¹³ Despite decades of intense theoretical and experimental analysis, a number of questions regarding the time scale and mechanism for this fundamental biomolecular process remain open.

A number of theoretical models have been developed to estimate the rate of helix formation as a function of s and σs (or H and J) for the ZB model. In an early and seminal paper, Schwartz¹⁴ estimated that, at the midpoint in the coil-to-helix transition, the mean time for helix formation reaches a maximum given by

$$\tau = \frac{1}{4\sigma k_F} \quad (3)$$

where k_F is the rate of adding an additional helical residue at the helix end. Interpreting a body of experimental studies, Zana⁸ estimated that k_F , the rate of addition of a single residue to a growing helix, was roughly 10^8 s^{-1} . That early work provided a simple initial relationship between the equilibrium energetic parameter σ and the rate of helix propagation k_F . More detailed calculations based on Schwartz's model were presented by Craig and Crothers¹⁵ and others. Subsequently, more detailed kinetic theories based on master equation approaches employing parameters derived from equilibrium analysis using the ZB model were developed. An example is the work of Gō who employed a master equation with transition elements based on a ZB model energetics.¹⁶ Properties of the relaxation near the equilibrium state were derived, and it was observed that the kinetic rate constant was a maximum when the ZB propagation constant s was unity. More elaborate explorations in a similar spirit are possible through a direct application of the kinetic Ising model.¹⁷

Brooks proposed a kinetic model based on a sequential formation of helical residues at a rate

$$k_+ \sim e^{-\beta\Delta G^\ddagger} 10^{12} \text{ s}^{-1} \quad (4)$$

On the basis of the results of extensive simulation studies of

terminally blocked polyalanine peptides, the equilibrium constant for nucleation of helix from coil was taken to be $\sigma s = \exp(-\beta\Delta G_n)$ with ΔG_n ranging from 3.1 to 3.7 kcal/mol; the equilibrium constant for propagation of a helical residue was taken $s = \exp(-\beta\Delta G_p)$ with ΔG_p ranging from -0.24 to -0.06 kcal/mol near room temperature; the barrier to addition of a single residue to an existing helix was estimated to be $\Delta G^\ddagger = 2.8$ kcal/mol. Brooks demonstrated that the mean time for the kinetic process of helix folding/unfolding scaled as

$$\tau \approx \frac{1}{\sigma} \quad (5)$$

for peptides forming up to 15 α -helical bonds, in agreement with the theory of Schwartz^{14,18,19}. Moreover, fits of the proportionality constant showed that $k_F \sim 6 \times 10^9 \text{ s}^{-1}$ in close agreement with $k_+ = 8 \times 10^9 \text{ s}^{-1}$ at 298 K. The analysis of Brooks agrees with the scaling law of Schwartz and, employing results from energetics derived from simulation, provides microscopic estimates of the σ and k_F parameters. Moreover, the analysis led to the important conclusion that the time scale for the process of helix folding and unfolding could occur on the nanosecond time scale. In a recent extension of that work, Weaver has demonstrated that for a slightly modified version of the sequential kinetic model of Brooks it is possible to evaluate the helix-to-coil probability distribution as a function of time and temperature for a diffusive dynamics.^{20,21}

Thompson et al. subsequently put forward a "kinetic zipper" model of the helix folding and unfolding kinetics. Their model sought to relax key assumptions inherent to the models of Schwartz, that estimated the mean time for formation of an *average* helical residue ignoring end effects, and Brooks, that assumes nucleation can occur at a single site with propagation following sequentially from that site. Like the equilibrium zipper model, their kinetic zipper model assumed the existence of a single helical region in the peptide which is expected to be reasonable for short peptides. Using their model to fit experimental data for laser-induced temperature jump experiments on an alanine based polypeptide, they put forward several important conclusions. The helix growth rate was found to be on the order of 10^8 s^{-1} , an order of magnitude slower than the estimate of Brooks. The analysis justified their assumption that the rate of addition of a helical residue has an activation enthalpy of zero. Moreover, the values of σ resulting from their fits were on the order of 0.01, significantly larger than "standard" values ranging from 0.005 to 0.001.²

The recent temperature-jump transient infrared absorption experiments of Woodruff and co-workers²²⁻²⁴ on apomyoglobin (a 153 residue globular protein with eight strands of mostly α -helical segments) showed that the helix folding/unfolding relaxation rates are in the range of 10–160 ns. Those results agree with predictions of the kinetic model of Brooks¹⁰ showing that even simple and well parametrized statistical models can account for realistic estimations of the helix formation rates.

Inherent to each of the existing models of the kinetics of the coil-to-helix transition is one or a number of simplifying assumptions. For example, the kinetic zipper model assumes that helix propagates from a single nucleation site; the sequential kinetics model assumes that helix nucleation occurs at a single site in the peptide and propagates unidirectionally. As such, it is desirable to develop an alternative theory that would allow one to relax one or more of those assumptions. A particularly attractive approach is one based on the solution of a mean first-passage time equation²⁵⁻²⁷ that would implicitly allow for helix formation from multiple nucleation sites (important for longer

TABLE 1: Schematic Representation of the Relationship between Theories and Models for the Coil-to-Helix Transition Including the ZB (ZB) Model, the Ideal Two Level System (TLS) Model, the Theory of Zwanzig, Szabo and Bagchi (ZSB), and the AH Model from This Work

	equilibrium	dynamics
$J = 0$	TLS	ZSB
$J > 0$	ZB	AH

peptides and extension to larger σ values) and make no assumption regarding the number of helical regions or direction of helix propagation.

In a note on the kinetics of protein folding,²⁸ Zwanzig, Szabo, and Bagchi (ZSB) evaluated the mean first-passage time for the special case of a ZB-like model with no spin–spin coupling ($J = 0$). In the ZSB model, the mean first-passage time for the transition of the N independent two level systems of “native” and “coil” residues to an all native configuration was computed as a function of the energetic bias in favor of the native state (determined by the external field H). This can be considered to be an “ideal protein” model for a set of noninteracting amino acid residues. They found that a local bias of the native state configuration on the order of 1 kcal/mol could lead to “folding times” on the order of seconds for a chain of one hundred residues.

If we extend the ZSB model to the context of the coil-to-helix transition, we have lost something essential that was captured by the ZB model: the role of “cooperativity” in helix formation. When spin–spin coupling is ignored, the nucleation and propagation constants become equal $\sigma s = s = \exp(H)$. The model is that of an “ideal peptide” composed of N noninteracting residues. How can the site–site coupling be included in such a MFP time approach? It is well-known that a mean field approximation provides a simple means of deriving an approximate solution for the partition function of an Ising model (which can also, in one dimension, be computed exactly). The mean field approximation results in an effective single residue energy function where each spin interacts with an “average spin” representing the average spin state of the system. A set of self-consistent equations are solved by iteration to determine the partition function for the system. The mean field approximation captures the general features of the cooperative nature of helix formation through an energetics that is intermediate to that of the “ideal peptide” model of ZSB and the exact ZB model (see Table 1).

In this paper, we employ a mean field approximation to derive mean first-passage times for helix formation from the ZB model (the one-dimensional Ising model) as a function of the nucleation, σs , and propagation, s , parameters (J and H). Unlike the standard mean field approximation described above, the “mean sequence” approximation underlying our “active helix” (AH) model leads to a generalized mean first-passage time equation where the transition rates depend on the state of the system, a fundamental difference between the AH model and standard kinetic models based on a master equation with fixed state-to-state transition rates. The solution of a set of self-consistent kinetic equations leads to a complete description of the kinetic and equilibrium properties of the model including the dependence of the MFP time for helix formation and equilibrium helicity in terms of σ , s , and N . The equilibrium properties of the AH model are compared with those of the ZB model and the “zipper” model. The kinetic properties of the AH model are compared with those of the kinetic models of ZSB, the kinetic zipper model, and the sequential kinetics of Brooks. The results show that our model leads to realistic estimates for the

equilibrium and kinetic properties of helix formation in peptides. This AH model provides a new understanding of the detailed chain dynamics and the relation between microscopic interaction parameters and macroscopic equilibrium properties.

2. Mean First-Passage Times for Unimolecular Reactions

Many processes can be modeled as unimolecular reactions. Let us consider a simple model for the helix–coil transition where N is the total number of residues in a peptide, c is the number of residues in a coil state, and $N - c$ is the number of residues in a helical state. We consider the “reaction”



where k_0 and k_1 are the transition rates for the individual residues that are changing from a coil to a helical state. In the ZSB model, the individual rates k_0 and k_1 were assumed to be independent of the conformational state of the surrounding peptide. In the general case, the actual values of the transition rates depend on the state of the entire peptide. To capture that essential character, we consider mean transition rates $\bar{k}_0(c)$ and $\bar{k}_1(c)$ that are functions of the number c of coil residues of a peptide that is N residues long.

For such a model, one can write the backward master equation

$$\begin{aligned} \partial_t P(c, t) = & (N - c + 1)\bar{k}_0(c - 1)P(c - 1, t) + \\ & (c + 1)\bar{k}_1(c + 1)P(c + 1, t) - (N - c)\bar{k}_0(c)P(c, t) - \\ & c\bar{k}_1(c)P(c, t) \quad (7) \end{aligned}$$

The corresponding equation for the first-passage times is

$$\begin{aligned} (N - c)\bar{k}_0(c)[\tau(c + 1) - \tau(c)] + \\ c\bar{k}_1(c)[\tau(c - 1) - \tau(c)] = -1 \quad (8) \end{aligned}$$

Equation 8 can be derived by considering a simple jump process.²⁷ Suppose that the system of N residues has c residues in the coil state and $N - c$ residues in the helical state. In the time interval Δt that corresponds to the next jump, the probability that the system will move toward a number $c + 1$ of coil states is $(N - c)\bar{k}_0(c)\Delta t$. The probability that the system will move toward a number $c - 1$ of coil states is $c\bar{k}_1(c)\Delta t$. Therefore, the probability that the system will remain in the same state is $1 - (N - c)\bar{k}_0(c)\Delta t - c\bar{k}_1(c)\Delta t$. Using these results, the mean first-passage time for the system to move from the initial state, with c coil residues, to a final state with more helical residues can be written as

$$\begin{aligned} \tau(c) = \Delta t + (N - c)\bar{k}_0(c)\Delta t\tau(c + 1) + c\bar{k}_1(c)\Delta t\tau(c - 1) + \\ [1 - (N - c)\bar{k}_0(c)\Delta t - c\bar{k}_1(c)\Delta t]\tau(c) \quad (9) \end{aligned}$$

This result can be rewritten as the mean first-passage time eq 8 and does not depend on the size of the jump time step Δt .

Equation 8 can be solved as shown in the Appendix, and the general solution is

$$\tau(c) = \frac{1}{N} \sum_{n=a}^{c-1} \binom{N-1}{n}^{-1} \sum_{m=n+1}^b \binom{N}{m} \frac{1}{\bar{k}_0(m)} \prod_{l=n+1}^m K(l) \quad (10)$$

where $\binom{n}{k} = n!/k!(n - k)!$, $K(l) = \bar{k}_0(l)/\bar{k}_1(l)$, a and b are the positions of the boundaries (see the Appendix), and N is the total number of residues. This result is a generalization of the more common case that is found when the ratio of the mean

transition rates is constant and independent of c . In that special case, with the conditions $a = 0$ and $b = N$, the above expression reduces to

$$\tau(c) = \frac{1}{Nk_0} \sum_{n=0}^{c-1} \binom{N-1}{n}^{-1} \sum_{m=n+1}^N \binom{N}{m} K^{m-n} \quad (11)$$

which is the result obtained for the special case of the ZSB model.²⁸ Our result provides a closed form solution for the MFP time in the case of a cooperative transition where the local rates of transition are dependent on the state of the system. That is the case in many cooperative phenomena including the coil-to-helix transition in polypeptides and many examples of protein folding.

3. Calculation of the Mean Transition Rates

The most important feature of our approach is that the transition rates are dependent on the state of the peptide and the fraction of helical residues $(N - c)/N$. For a given peptide, a local transition from coil-to-helix is more probable when there are existing helical regions than when they are absent. In general, the local transition rates cannot be considered to be constants independent of the local peptide structure or coil content c . The case of transition rate *constants* is singular and can be considered only as an approximation for relaxation of the nonequilibrium system. In the general case, we can expect the ratio of the mean transition rates $\bar{k}_0(c)$ and $\bar{k}_1(c)$ to depend on c as $K(c) = \bar{k}_0(c)/\bar{k}_1(c)$. In this work, we will always consider that the transition rates and their ratio depend on c . For notational compactness, we do not always note that dependence explicitly.

In calculating the mean first-passage time using eq 10, we must evaluate mean transition rates and their ratio K . In this work, we invoke a mean-field or “mean-sequence” approximation. The mean transition rates \bar{k}_0 and \bar{k}_1 are defined by the probabilistic relations

$$\bar{k}_0^T = \frac{\sum_{\alpha} k_{h\alpha \rightarrow c\alpha} P_{h\alpha}}{\sum_{\alpha} P_{h\alpha}} \quad \bar{k}_1^T = \frac{\sum_{\alpha} k_{c\alpha \rightarrow h\alpha} P_{c\alpha}}{\sum_{\alpha} P_{c\alpha}} \quad (12)$$

for sites at the peptide’s N- and C-terminal ends (with one nearest neighbor residue) and

$$\bar{k}_0^I = \frac{\sum_{\alpha\beta} k_{\alpha h\beta \rightarrow \alpha c\beta} P_{\alpha h\beta}}{\sum_{\alpha\beta} P_{\alpha h\beta}} \quad \bar{k}_1^I = \frac{\sum_{\alpha\beta} k_{\alpha c\beta \rightarrow \alpha h\beta} P_{\alpha c\beta}}{\sum_{\alpha\beta} P_{\alpha c\beta}} \quad (13)$$

for sites that are interior (with two nearest neighbor residues), where the indices $\alpha, \beta \in \{c, h\}$.

The *uniresidue* conformational transition rates ($k_{hh \rightarrow ch}$, $k_{ccc \rightarrow ch}$, and so on) and the microscopic neighbor-dependent configurational probabilities (P_{hh} , P_{hhh} , and so on) can be calculated by proposing a specific model for the interresidue interactions in the polypeptide. As mentioned in the Introduction, in this work we employ the energetic model of Zimm and Bragg.

3.1. The Active Helix Ising Model. We consider the Ising model Hamiltonian, but with spins 0 (coil) and 1 (helix). Only the helical residues are “active” in the sense that the coil residues are not responsible for interactions with an external field or with any other residues. This is equivalent to transforming the original

± 1 spin values as

$$s_i \rightarrow \frac{s_i + 1}{2} \quad (14)$$

The energies of the available states are

$$E_{cc} = 0 \quad E_{ch} = E_{hc} = -H \quad E_{hh} = -J - 2H \quad (15)$$

for the N- and C-terminal sites and

$$E_{ccc} = 0 \quad E_{chc} = E_{cch} = E_{hcc} = -H \quad E_{hch} = -2H \\ E_{chh} = E_{hhc} = -J - 2H \quad E_{hhh} = -2J - 3H \quad (16)$$

for interior sites. Note that an important feature of our model, hereafter the AH Ising model, is that the energies of the *ccc* and *hhh* configurations are extreme values if $H < 0$ (as is needed to obtain physically relevant values for σ and s for the coil-to-helix transition) and $J > -3H/2$. In such a case, the coil-to-helix transition is modeled as a simple deexcitation to the bounded ground state of the system *hhh*. In general, however, the kinetics of the system will be dictated by the relative values of the energetic parameters that enter the energetics of the ZB Ising Hamiltonian (eq 1).

Within this model, the transition rates are given by the general expression

$$k_{a \rightarrow b} = \frac{kT}{h} e^{\Delta S/k} e^{-\beta \Delta E_{ab} \Theta(\Delta E_{ab})} = \nu e^{-\beta \Delta E_{ab} \Theta(\Delta E_{ab})} \quad (17)$$

where $\Theta(x)$ is the Heaviside function which is unity for $x \geq 0$ and zero otherwise. As a result, we always have $k_{a \rightarrow b} = \nu$ if $\Delta E_{ab} \leq 0$, where ν is the standard transition frequency of unimolecular rate theory. We use a value of $\nu = 10^9$ as was suggested by Zana⁸ and used by ZSB in another context.²⁸ To simplify the calculations, we have introduced the notation $\theta \equiv (N - c)/N = 1 - \theta_c$ for the helical fraction (with θ_c being the fraction of coil residues), $e^{-\beta J} \equiv e_J$ and $e^{-\beta H} \equiv e_H$. The uniresidue conformational transition rates are

$$k_{hc \rightarrow cc} = \nu e_H^{\Theta(H)} \quad k_{hh \rightarrow ch} = \nu (e_J e_H)^{\Theta(J+H)} \\ k_{cc \rightarrow hc} = \nu e_H^{-\Theta(-H)} \quad k_{ch \rightarrow hh} = \nu (e_J e_H)^{-\Theta(-(J+H))} \quad (18)$$

for transitions by the terminal residues and

$$k_{chc \rightarrow ccc} = \nu e_H^{\Theta(H)} \quad k_{chh \rightarrow cch} = k_{hhc \rightarrow hcc} = \nu (e_J e_H)^{\Theta(J+H)} \\ k_{hhh \rightarrow hch} = \nu (e_J^2 e_H)^{\Theta(2J+H)} \quad k_{ccc \rightarrow chc} = \nu e_H^{-\Theta(-H)} \\ k_{cch \rightarrow chh} = k_{hcc \rightarrow hhc} = \nu (e_J e_H)^{-\Theta(-(J+H))} \\ k_{hch \rightarrow hhh} = \nu (e_J^2 e_H)^{-\Theta(-(2J+H))} \quad (19)$$

for transitions at interior residues.

These rates can be used in eqs 12 and 13, together with the configurational probabilities that are derived in the next section, to calculate the *mean* transition rates for conformational transitions.

3.2. The Neighbor-Dependent Configurational Probabilities. A realistic model for the conditional probabilities must take into account the fact that, once the neighbors of the residue of interest are fixed, the residue can access only a finite number of energetic states. As a result, the probability of that residue being coil or helix should be calculated differently than the probabilities for its neighbors. For example, the probabilities

P_{hhh} and P_{hh} are taken to be

$$P_{hhh} = P_h^n P_h^l P_h^n \quad P_{hh} = P_h^T P_h^n \quad (20)$$

For the neighbors

$$P_h^n = \frac{N-c}{N} = \theta \quad (21)$$

but for the internal or for the N- and C-terminal residues

$$P_h^l = \frac{1}{1 + e^{-\beta(2J+H)}} \quad P_h^T = \frac{1}{1 + e^{-\beta(J+H)}} \quad (22)$$

where we assign the “all helix” energy configurations (E_{hhh} and E_{hh}) to be the reference levels. Therefore

$$P_{hhh} = \frac{\theta^2}{1 + e^{-\beta(2J+H)}} \quad P_{hh} = \frac{\theta}{1 + e^{-\beta(J+H)}} \quad (23)$$

Other probabilities can be calculated in the same manner leading to the conditional probabilities

$$P_{hc} = (1 - \theta)/(1 + e_H) \quad P_{cc} = (1 - \theta)e_H/(1 + e_H) \\ P_{hh} = \theta/(1 + e_H e_J) \quad P_{ch} = \theta e_H e_J/(1 + e_H e_J) \quad (24)$$

for the N- and C-terminal residues and

$$P_{hhh} = \theta^2/(1 + e_J^2 e_H) \quad P_{hch} = \theta^2 e_J^2 e_H/(1 + e_J^2 e_H) \\ P_{chc} = (1 - \theta)^2/(1 + e_H) \quad P_{ccc} = (1 - \theta)^2 e_H/(1 + e_H) \\ P_{chh} = P_{hch} = \theta(1 - \theta)/(1 + e_J e_H) \\ P_{cch} = P_{hcc} = \theta(1 - \theta) e_J e_H/(1 + e_J e_H) \quad (25)$$

for the interior sites, where the notation for e_J and e_H is the same as in the previous section. These probabilities are normalized as

$$\sum_{\alpha\beta\gamma} P_{\alpha\beta\gamma} = \sum_{\alpha\beta} P_{\alpha\beta} = 1 \quad (26)$$

where the indices $\alpha, \beta, \gamma \in \{c, h\}$.

3.3. The Mean Transition Rates. Using the conditional probabilities, defined in the previous section, and the relations $e^{-x\Theta(x)} = 1 + (e^{-x} - 1)\Theta(x)$ and $e^{x\Theta(-x)} = e^x e^{-x\Theta(x)}$, which hold for both negative and positive values of x , we obtain the mean configurational transition rates for the helix-to-coil (\bar{k}_0) and coil-to-helix (\bar{k}_1) for N- and C-terminal residues as

$$\bar{k}_0^T = \frac{\nu}{f_3}(f_1\Theta(J+H) + f_2\Theta(H) + f_3) \quad (27)$$

with the terms f_1 , f_2 , and f_3 given by

$$f_1(J, H, \theta) = (1 + e_H)(e_J e_H - 1)\theta \\ f_2(J, H, \theta) = (e_H - 1)(1 + e_J e_H)(1 - \theta) \\ f_3(J, H, \theta) = 1 + e_J e_H + e_H(1 - e_J)\theta \quad (28)$$

and

$$\bar{k}_1^T = \frac{\nu}{f_4}(f_1\Theta(J+H) + f_2\Theta(H) + f_3) \quad (29)$$

with

$$f_1(J, H, \theta) = (1 + e_H)(e_J e_H - 1)\theta \\ f_2(J, H, \theta) = (e_H - 1)(1 + e_J e_H)(1 - \theta) \\ f_3(J, H, \theta) = 1 + e_J e_H + e_H(1 - e_J)\theta \\ f_4(J, H, \theta) = e_H[1 + e_J e_H + (e_J - 1)\theta] \quad (30)$$

For interior residues the helix to coil (\bar{k}_0^I) mean transition rate is given by

$$\bar{k}_0^I = \frac{\nu}{f_4}(f_1\Theta(2J+H) + f_2\Theta(J+H) + f_3\Theta(H) + f_4) \quad (31)$$

with

$$f_1(J, H, \theta) = (1 + e_H)(1 + e_J e_H)(e_J^2 e_H - 1)\theta^2 \\ f_2(J, H, \theta) = 2(1 + e_H)(1 + e_J^2 e_H)(e_J e_H - 1)\theta(1 - \theta) \\ f_3(J, H, \theta) = (1 + e_J e_H)(1 + e_J^2 e_H)(e_H - 1)(1 - \theta)^2 \\ f_4(J, H, \theta) = (1 + e_J e_H)(1 + e_J^2 e_H) + \\ 2e_H(1 - e_J)(1 + e_J^2 e_H)\theta + e_H(1 - e_J)^2(e_J e_H - 1)\theta^2 \quad (32)$$

A similar relation can be derived for \bar{k}_1^I . Note that if $H < 0$ and $J < -H/2$ then $\Theta(H) = \Theta(J+H) = \Theta(2J+H) = 0$ and $\bar{k}_0^T = \bar{k}_0^I = \nu$. In this case, the rate of transformation from helix to coil is downhill and barrierless in our model, being a constant independent of θ . A similar assumption was introduced and tested by Thompson et al. in their kinetic zipper model. By design, \bar{k}_0 and \bar{k}_1 depend on θ .

We can calculate the global mean transition rate \bar{k}_0 , for the entire peptide, by averaging over the “end effects” and assuming that

$$\bar{k}_0 = \frac{2}{N}\bar{k}_0^T + \left(1 - \frac{2}{N}\right)\bar{k}_0^I \quad (33)$$

and

$$\bar{k}_1 = \frac{2}{N}\bar{k}_1^T + \left(1 - \frac{2}{N}\right)\bar{k}_1^I \quad (34)$$

The ratio of the transition rates is then

$$K(e_H, e_J, N, \theta) = \bar{k}_0/\bar{k}_1 \quad (35)$$

and is dependent on the interaction energies J and H and the helical fraction θ . For dipeptides ($N = 2$), K is dependent only on the dynamics of the *terminal sites*, whereas for long peptides ($N \rightarrow \infty$), K is dictated mainly by the dynamics of the *interior sites*.

The presence of the Heaviside functions $\Theta(2J+H)$, $\Theta(J+H)$, and $\Theta(H)$ in the transition rate formulas emphasizes the crucial role of the relative values of the interaction energies J and H in determining the specific kinetic properties of our system. The analytic expression for the mean transition rates that are derived here are exact (in the limits of our theoretical model) and can be easily evaluated computationally.

4. Mean First-Passage Time for the Active-Helix Ising Model

By using the mean transition rates derived in section 3.3, we can calculate numerically the mean first-passage times as a function of the energetic parameters J and H (or later σ and s).

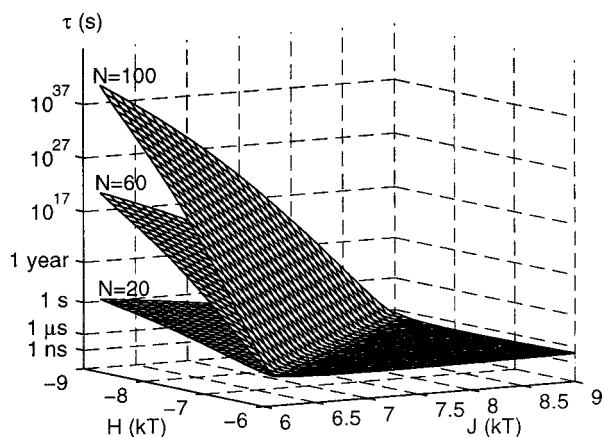


Figure 1. “All coil” to “all helix” MFPT calculated as a function of the interaction energies J and H for peptides of length $N = 20, 60,$ and 100 and the initial fraction of coil residues $\theta_c = 1$. Note that the time units are seconds (unless specifically stated otherwise, for convenience) and $1 \text{ year} \approx 10^{7.5} \text{ s}$.

Figure 1 shows the 2D surfaces representing the mean first-passage times calculated for peptides that are $N = 20, 60,$ and

100 residues long. In this figure, as well as in Figures 2–8, we considered the transition to the “all helix” final states. It is possible, however, to calculate the MFP time using the general result of eq 10 with various values of the boundary conditions a and b that correspond to situations of interest for theoretical calculations or for actual experiments.

The general features of the MFP time depend on both J and H . As expected, the H dependence of the MFP time is similar to that obtained by ZSB²⁸ in that there is a decrease in the MFP time for increasing values of the relative stabilization of the helical state relative to the coil state. However, there is an important difference. In our AH model, the MFP time depends on both the J and H interaction energies. To obtain physically reasonable helix folding times we consider $H < 0$ meaning that for an *isolated* residue (in the absence of interresidue hydrogen bonding) the coil state is more stable than the helix configuration, as expected. We find that biologically relevant MFP times, on the time scale of nanoseconds to microseconds, can be obtained by increasing J as well as by increasing H . Even in the total absence of an external field bias ($H = 0$), the presence

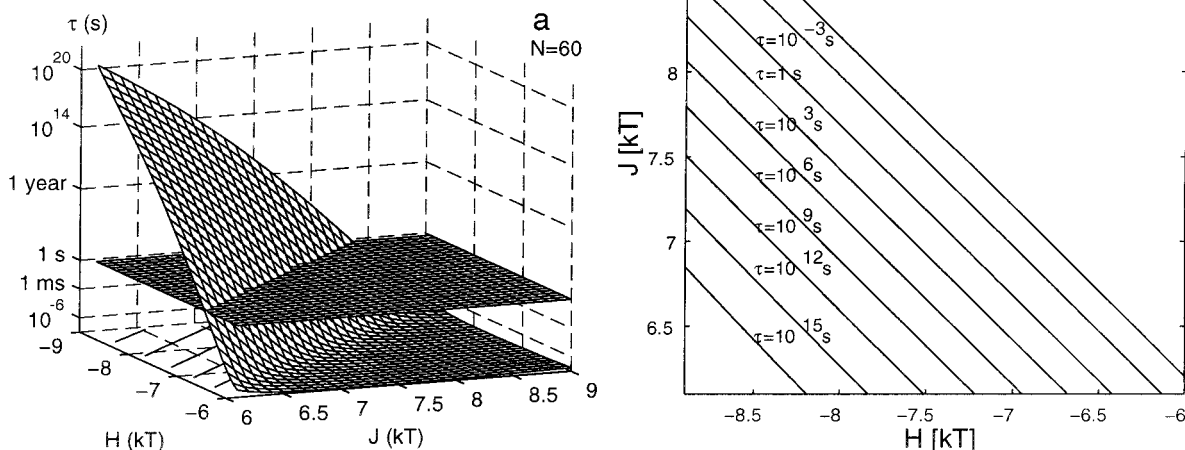


Figure 2. (a) MFPT (“all coil” to “all helix”) as a function of the interaction energies J and H for $N = 60$ and the initial fraction of coil residues $\theta_c = 1$. Note that the time units are seconds (unless specifically stated otherwise, for convenience), $1 \text{ year} \approx 10^{7.5} \text{ s}$. (b) The solid lines are the corresponding contours of constant values of the MFPT.

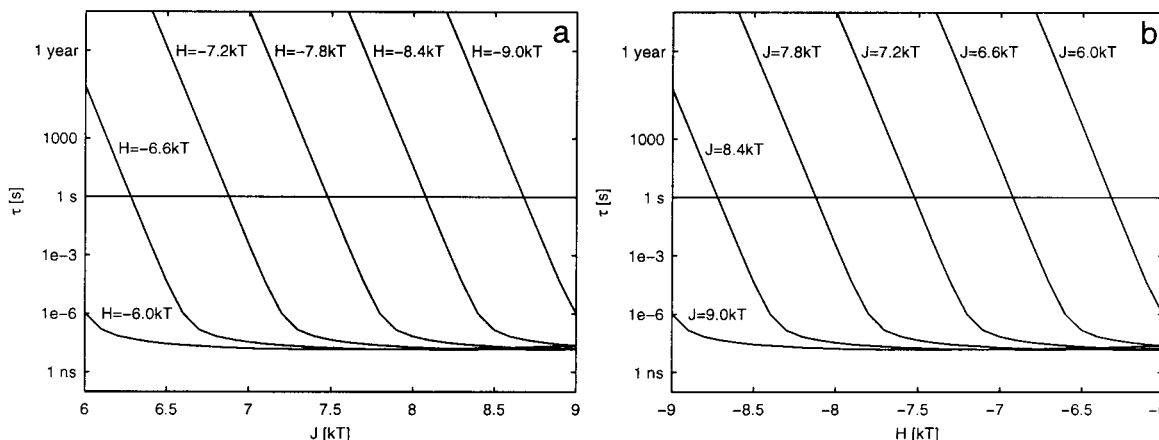


Figure 3. MFPT (transition to “all helix”) as a function of the interaction energies J and H ($N = 100$ and $\theta_c = 0.34$). Note the strong dependence of the MFPT on both interaction energies J and H . For a strong external field H , equally strong residue–residue interactions J of opposite sign are necessary to reach coil-to-helix transitions faster than 1 s. Because of the exponential dependence of τ on J and H , small variations of the interaction energies can account for dramatic changes in the MFPT.

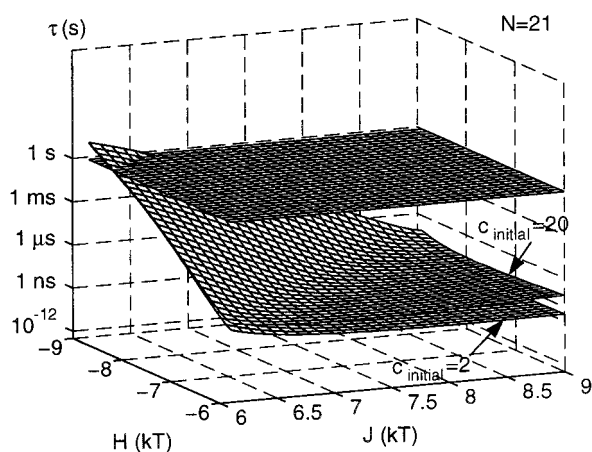


Figure 4. Transition to “all helix”, MFPT for $N = 21$. The upper surface corresponds to an initial state with 20 coil residues, and the calculated MFPT values are therefore larger than for the case $c_{\text{initial}} = 2$ represented by the lower surface.

of a small interresidue J interaction on the order of kT can lower the MFP time for the coil-to-helix transition well below one second.

Figure 2 focuses on the $N = 60$ surface. The solid lines in Figure 2b are the equitemporal contours of the data presented in Figure 2a corresponding to constant values of the MFP time. The results presented in this plot demonstrate that physically

reasonable time scales for helix folding can be found for a range of values of the energetic parameters H and J (or correspondingly s and σ). The result of ZSB demonstrated that time scales for protein folding on the order of seconds or less could be achieved through a small local bias in the uniresidue energetics toward the native configuration state (corresponding to positive values of H). As a generalization of that observation, we find that physically reasonable time scales for helix folding can be achieved through an increase in the favorable interresidue hydrogen bonding stabilization interaction (through positive values of J) which overcomes a local uniresidue energetic bias in favor of the coil configuration (through negative values of H).

Cross sections of the data presented in Figure 2 are shown in Figure 3 for an $N = 100$ polypeptide. We find that for a strong external field H equally strong residue–residue interactions J of opposite sign are necessary to reach coil-to-helix transitions in a mean time less than 1 s through stabilization of interresidue interactions. Note that even relatively small variations of the interaction energies can account for very dramatic changes in the MFP time.

In Figure 4, we show the dependence of the MFPT of an $N = 21$ polypeptide as a function of J and H . Consistent with the early observations of Brooks,¹⁰ but dependent on our choice of the reaction “frequency factor”, for small polypeptides the MFPT can occur in the nanosecond time scale. Figure 4 demonstrates the dependence of τ on the initial state of the peptide. The upper surface corresponds to an initial state with 20 coil residues. The

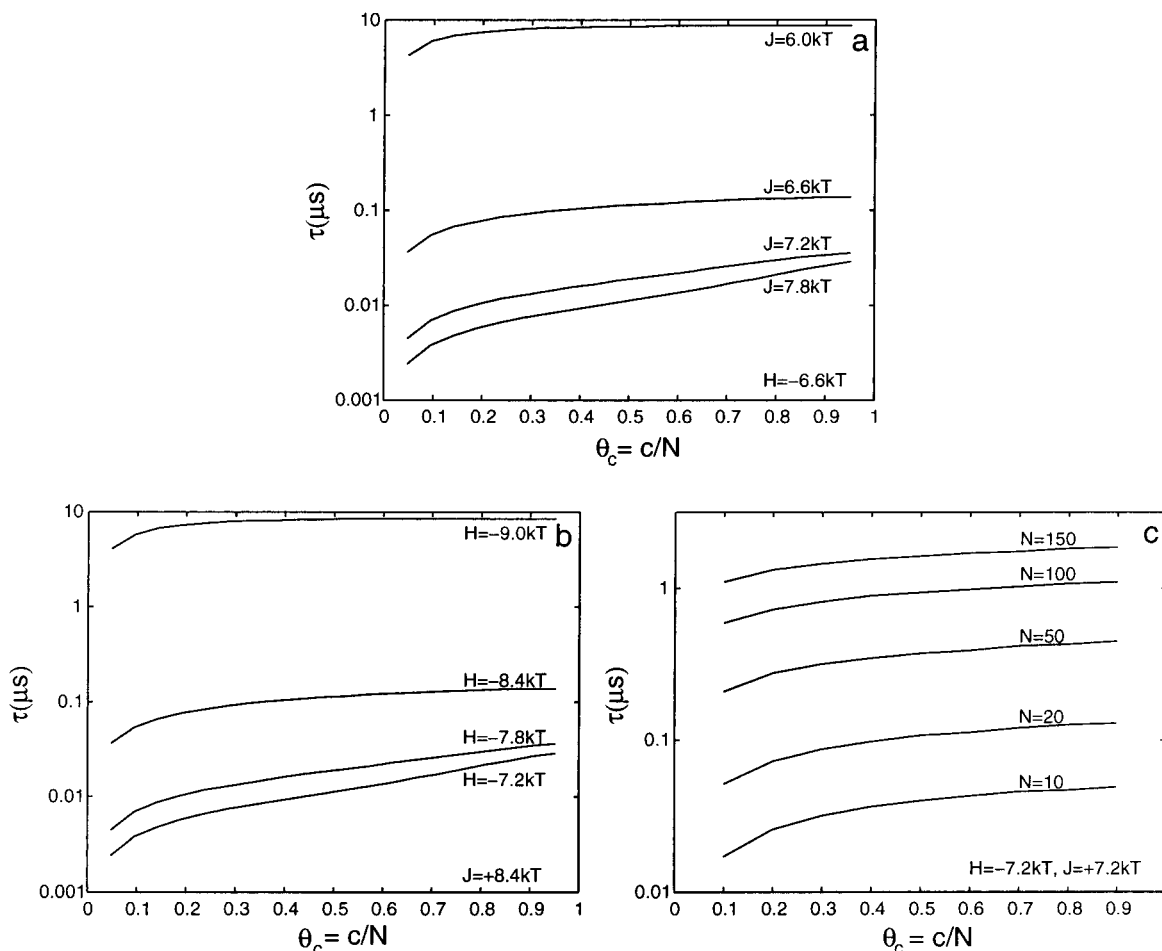


Figure 5. MFPT (transition to “all helix”) as a function of the fraction of coil, $\theta_c = 1 - \theta$, for various values of J , H , and N . (a) J is varied with $N = 21$ and $H = -6.6kT$; (b) H is varied with $N = 21$ and $J = 8.4kT$; (c) N is varied with $H = -7.2kT$ and $J = 7.2kT$. As the number of residues in the coil state increases (θ_c close to 1) so does the MFPT. The MFP time increases exponentially with the length of the peptide N .

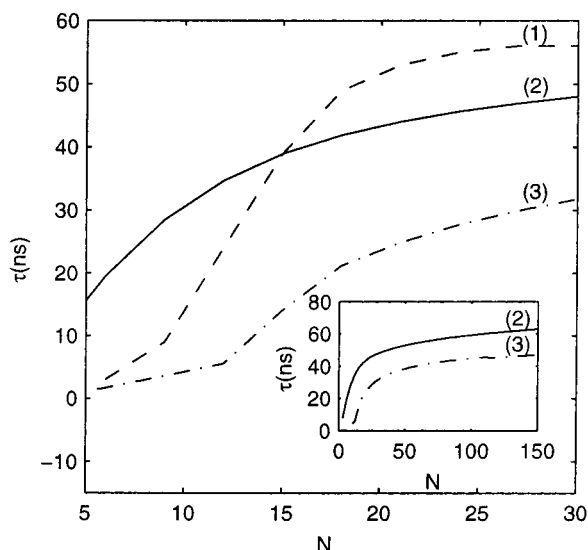


Figure 6. Comparison between our calculated values for the MFP time (τ), using the AH model, and the values for the helix folding times calculated by Brooks.¹⁰ The dashed curve numbered 1 is the result of Brooks, whereas the curves numbered 2 (solid) and 3 (dash-dot) are calculated for the same σ and s parameters using our AH model. In the AH model, N is the length of the peptide (the final number of residues in a helical state for the coil-to-helix transition). We have accounted for the fact that in Figure 3 of Brooks¹⁰ N corresponds to the number of helical hydrogen bonds.

calculated MFPT values are therefore larger than those for the case of two initial coil residues represented by the lower surface.

Another important aspect of our AH model is that it permits quantitative estimates of the dependence of the MFP time on all parameters important in describing the peptide folding including J , H , θ , and N . For example, Figure 5 shows the dependence of the MFP time on the fraction of coils θ_c as a function of the length of the chain (N) for various values of the interaction energies J and H . Note that physically reasonable MFP times, similar to the ones recently reported by Thompson and Eaton,^{11,29,30} are estimated from our calculations. In Figure 5a, we vary J for $N = 21$ and $H = -6.6kT$; in b, we vary H for $N = 21$ and $J = 8.4kT$; in c, we vary N for $H = -7.2kT$ and $J = 7.2kT$. Note that longer MFP times are obtained in all of the cases when the number of residues in the coil state is increased (θ_c close to 1).

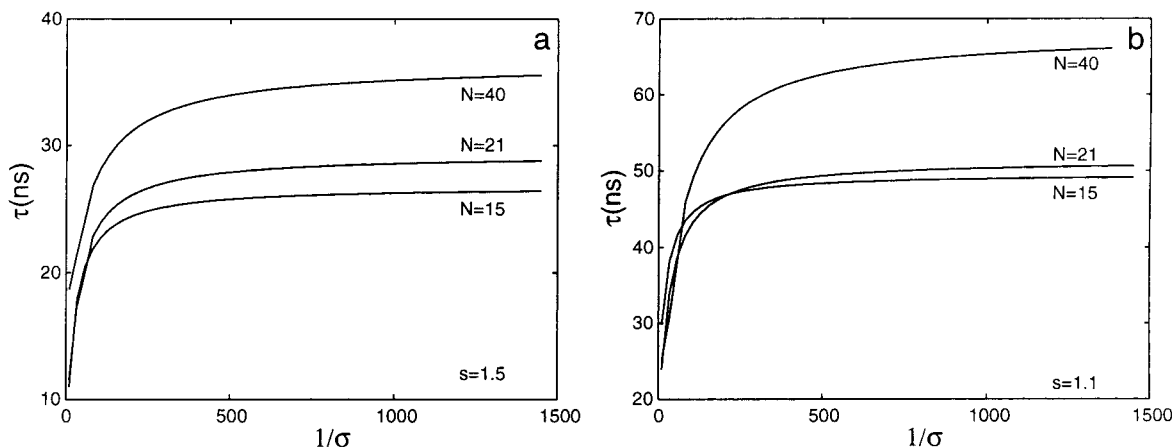


Figure 7. Predictions of the AH model for the MFPT, for the all coil to all helix transition, plotted as a function of $1/\sigma$ for (a) $s = 1.5$ and (b) $s = 1.1$, for varying lengths of the polypeptide. Note that in the more cooperative case, $s = 1.5$, the N dependence is least pronounced. As has been noted by others, and as is explicit in the scaling law of Schwartz, the MFP time increases monotonically with decreasing values of the nucleation parameter σ . Note that for large values of σ there is a strong nonlinear behavior because of the increasing importance of multinucleation pathway in the coil-to-helix transition.

In Figure 6 is shown the dependence of the MFP time on the length of the polypeptide N . Shown for comparison is the data of the “sequential” kinetics model taken from Figure 3 of Brooks¹⁰ ($\sigma = 0.002$ and $s = 1.5$). The dashed curve numbered 1 is the result of Brooks, whereas the curves numbered 2 (solid) and 3 (dash-dot) are calculated for the same σ and s parameters using our AH model. The J and H values that are necessary for the MFP time calculation were estimated using eq 2. The solid curve 2 was calculated for the “all coil” to “all helix” transition, corresponding to the boundary conditions $a = 0$ and $b = N$ in eq 10. Curve 3 was obtained for the case when the transition is considered to take place between the “all coil” and equilibrium states, corresponding to $a = (1 - \theta_{eq})N$ and $b = N$; in the next section is explained how we obtained the equilibrium fraction of helical residues θ_{eq} (eq 42). We note that both types of calculations show similar characteristics of the MFP time dependence on N . The times for transition to the equilibrium fraction of helix, curve 3, correspond to lower values than the times for transition to all helix, curve 2, as expected. Our results show the qualitative features of a two-phase kinetic behavior, consisting of an initial rapid rise and subsequent slower increase in the MFP time τ with increasing N . Note that τ continues to increase with N for large N (see the inset) as would be expected on physical grounds and shows no plateau at large N . When compared with the data of Brooks, the dependence of τ on N in the AH model shows a more diffuse, less sigmoidal or cooperative transition with increasing N .

In Figure 7 we investigate the MFPT dependence for $N = 15, 21,$ and 40 on $1/\sigma$ for $s = 1.5$ and 1.1 . The mean relaxation time τ_M^* predicted by Schwartz and Seeling is found to scale as $\tau_M^* \sim (4\sigma k_F)^{-1}$. Note that, for large values of σ , there is a strongly nonlinear dependence on $1/\sigma$. This results from the inclusion in our AH model of the possibility of helix formation through a mechanism involving multiple nucleation sites. As expected, the effect is increasingly important as the length of the peptide N increases. For smaller values of σ , we find a fairly weak but distinct sensitivity of the MFP time to variations in σ . Moreover, the multiple nucleation mechanism is seen to be increasingly important for longer polypeptides and smaller values of the propagation constant s .

The dependence of the rate of helix formation on the propagation constant s has been explored by Gō and others. For the kinetic rate constant (a sum of folding and unfolding

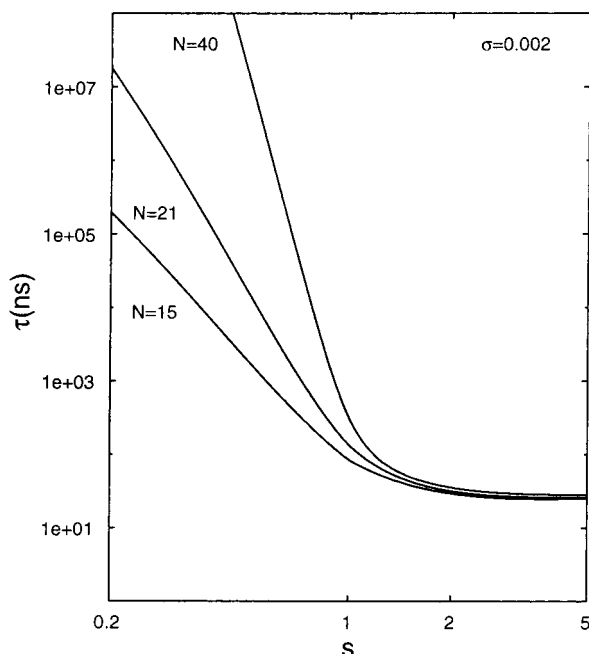


Figure 8. Predictions of the AH model for the MFPT, for the all coil to all helix transition, as a function of s for polypeptides for $\sigma = 0.002$ and $N = 21$. As expected for the coil-to-helix transition, the mean first-passage time is a monotonically decreasing function of s .

rates), the relaxation time for the approach to equilibrium was found to be a maximum near $s = 1$. For our study, we have focused on the forward coil-to-helix transition process. In Figure 8, we show the dependence of the MFP time for that process as a function of the helical propagation parameter s . As expected, the MFP time decreases monotonically as s is increased and the forward propagation of helix is enhanced. If we were to consider the reverse process (that of the MFP time of the helix to coil transition), we expect to find the opposite behavior manifest in a monotonically increasing τ with increasing s . As such, the overall kinetic rate constant, which can be approximated by the sum of the inverse MFP times for these two processes, is expected to show a maximum near $s = 1$ consistent with the results of $G\bar{\sigma}^{16}$.

5. Equilibrium Properties. Validation of the Active-Helix Ising Model.

To compare our AH model to the ZB model, we derive the equivalent equilibrium fraction of helix as a function of the *nucleation* (σs) and *propagation* (s) parameters. For the *propagation* step, the mean sequence uniresidue transition rates are given by

$$\begin{aligned} \bar{k}_1^T &= k_{\underline{c}h \rightarrow \underline{h}h} & \bar{k}_0^T &= k_{\underline{h}h \rightarrow \underline{c}h} \\ \bar{k}_1^I &= \frac{1}{\gamma} \sum_{\alpha\beta}^* k_{\alpha\underline{c}\beta \rightarrow \alpha\underline{c}\beta} P_{\alpha\underline{h}\beta} & \bar{k}_0^I &= \frac{1}{\gamma} \sum_{\alpha\beta}^* k_{\alpha\underline{h}\beta \rightarrow \alpha\underline{c}\beta} P_{\alpha\underline{h}\beta} \end{aligned} \quad (36)$$

where the restricted sum $\sum_{\alpha\beta}^* P_{\alpha\beta} = \gamma$ excludes the terms $\alpha = \beta = c$. For the *nucleation* step, the mean transition rates are given by

$$\begin{aligned} \bar{k}_1^T &= k_{\underline{c}\underline{c} \rightarrow \underline{h}\underline{c}} & \bar{k}_0^T &= k_{\underline{h}\underline{c} \rightarrow \underline{c}\underline{c}} \\ \bar{k}_1^I &= k_{\underline{c}\underline{c}\underline{c} \rightarrow \underline{c}\underline{h}\underline{c}} & \bar{k}_0^I &= k_{\underline{c}\underline{h}\underline{c} \rightarrow \underline{c}\underline{c}\underline{c}} \end{aligned} \quad (37)$$

By using the conditional probabilities derived in 3.2 and the

above mean transition rates for the propagation step, we can build the *propagation* equilibrium fraction “ s ”, defined as

$$s^T = \bar{k}_1^T / \bar{k}_0^T \quad s^I = \bar{k}_1^I / \bar{k}_0^I \quad (38)$$

In a similar way, we can build the *nucleation* equilibrium fraction “ σs ” for *internal* and *terminal* sites

$$\sigma s^T = \bar{k}_1^T / \bar{k}_0^T \quad \sigma s^I = \bar{k}_1^I / \bar{k}_0^I \quad (39)$$

Averaging over end effects, we write

$$\begin{aligned} s &= \frac{2}{N} s^T + \left(1 - \frac{2}{N}\right) s^I \\ \sigma s &= \frac{2}{N} \sigma s^T + \left(1 - \frac{2}{N}\right) \sigma s^I \end{aligned} \quad (40)$$

At equilibrium, $K = c/(N - c) = (1 - \theta)/\theta$. Using eq 35 for K derived in our model by averaging over the uniresidue transition rates, we expect that at equilibrium

$$K(e_H, e_J, N, \theta) = \frac{1 - \theta}{\theta} \quad (41)$$

where the solution is written $\theta_{\text{eq}} = \theta_{\text{eq}}(e_H, e_J, N) = \theta_{\text{eq}}(J, H, N)$. To compare the behavior of the AH model with the ZB results, eqs 35 and 40 can be used to find the numerical relation

$$\theta_{\text{eq}} = \theta_{\text{eq}}(s, \sigma) \quad (42)$$

In Figure 9 is shown a comparison between our calculated values for σ and s , using the AH model, and the approximation used by Bryngelson and Billings and shown in eq 2. In this case, for $N = 21$, we find that very good correlations are observed facilitating our equilibrium calculations. However, for larger peptides, important differences may be obtained when using the approximate eq 2 as opposed to eq 40.

In Figure 10 are shown the θ vs s diagrams calculated for our AH model for (a) $N = 20$, (b) $N = 100$, and (c) $N = 1000$. To obtain the equilibrium values of the fraction of helical residues we devised an iterative procedure that starts from initial σ and s values and an initial guess for the number of coil residues at equilibrium (say $c_{\text{ini}} = 2$). Because of the good correlations depicted in Figure 9, eq 2 can be used to estimate the corresponding values of J and H . These values are then used in eq 35 to calculate K exactly which provides a new estimate for the equilibrium fraction of coil $\theta = 1/(1 + K)$ and a new number of coil residues $c = (1 - \theta)N$. The modified values are then reintroduced. This iterative algorithm converges to the equilibrium fraction of helix θ that is shown in the diagrams of Figure 10. These diagrams are in very good agreement with the predictions of the ZB model, suggesting that our choice of configurational probabilities based on the mean sequence approximation leads to realistic equilibrium properties of the AH model. The $N = 100$ diagram is essentially identical to the results of the ZB theory.

The iterative procedure was used to obtain the equilibrium fraction of helical residues. We used the values of J and H that correspond to the values of σ and s used by Brooks. For each value of N , we used eq 41 to estimate the equilibrium fraction of coil. Given the equilibrium fraction of coil, we defined the position of the absorbing boundary condition $a = (1 - \theta_{\text{eq}})N$ and calculated the MFP time using eq 10 (as explained in the previous section).

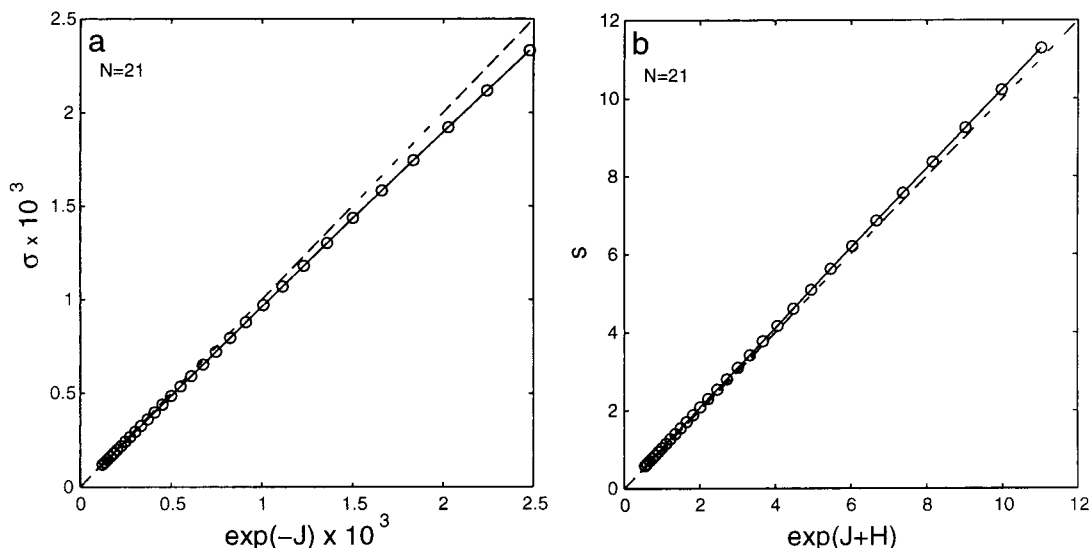


Figure 9. Comparison between our calculated values for σ and s , using the AH model, and the approximation used by Bryngelson and Billings $\sigma = e^{-J}$ and $s = e^{J+H}$. In this case of $N = 21$, very good correlations are observed that facilitate our equilibrium calculations (see text for details).

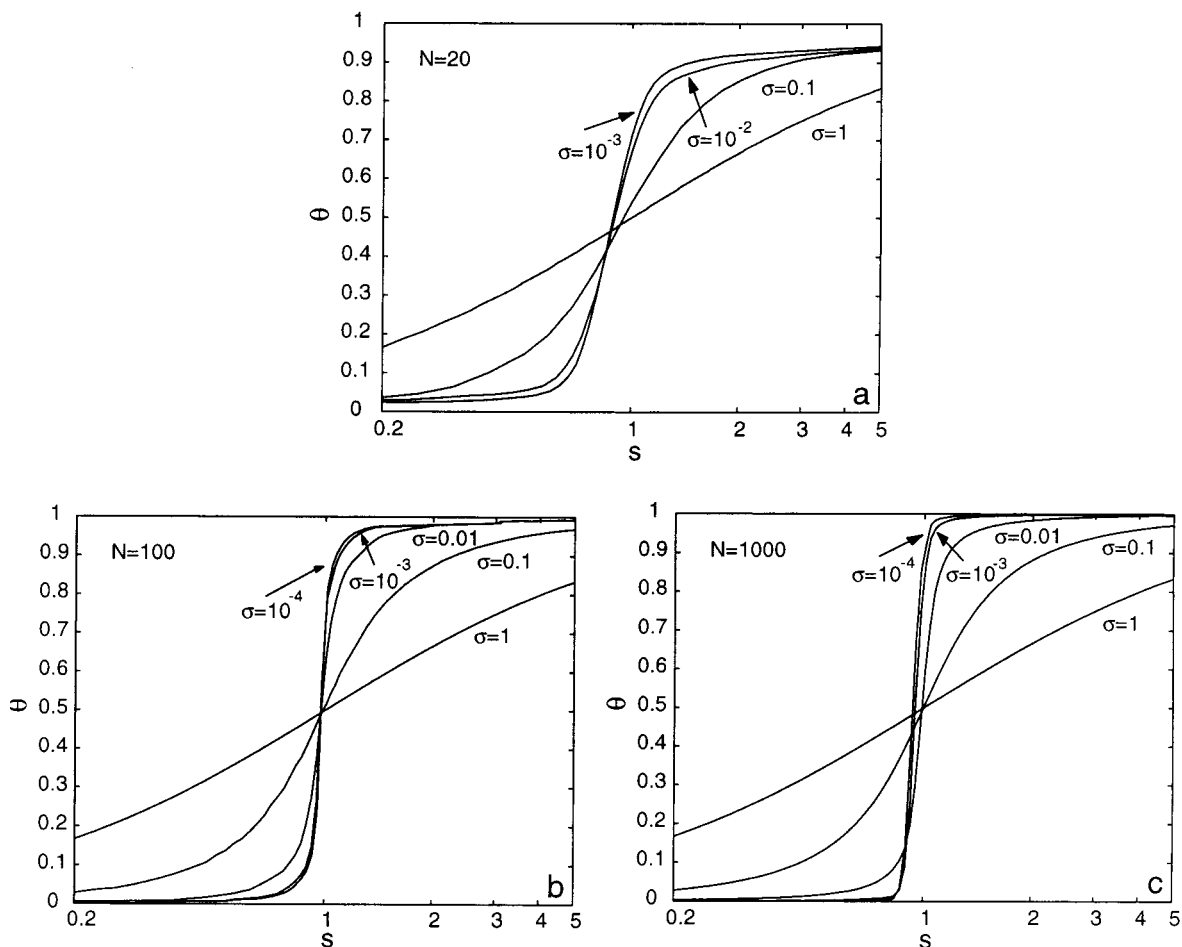


Figure 10. θ vs s diagram calculated for our AH model for (a) $N = 20$, (b) $N = 100$, and (c) $N = 1000$. These diagrams are in very good agreement with the predictions of the ZB model. The results show that our choice of configurational probabilities leads to realistic equilibrium properties of the AH model. The $N = 100$ diagram (b) is essentially identical to the result of the ZB theory.

Figure 11 shows the N vs s diagram calculated for our AH model and for the “zipper” model. For the results of the AH model, we used again the self-consistent iterative procedure described above, holding σ constant for peptides of various N . In the cases $\theta = 0.1, 0.3, 0.5, 0.7$, and 0.9 we explored the $N - s$ plane with an accuracy of $d\theta = \pm 0.02$. The averages were

plotted as solid lines. For the results corresponding to the “zipper” model, we used the well-known result to estimate the equilibrium values for θ^2 . The values of the nucleation parameter were for the AH model (a) $\sigma = 10^{-4}$ and for the zipper model (b) $\sigma = 10^{-1}$ and (c) $\sigma = 10^{-4}$. Good qualitative agreement with the predictions of the “zipper” model is observed. All

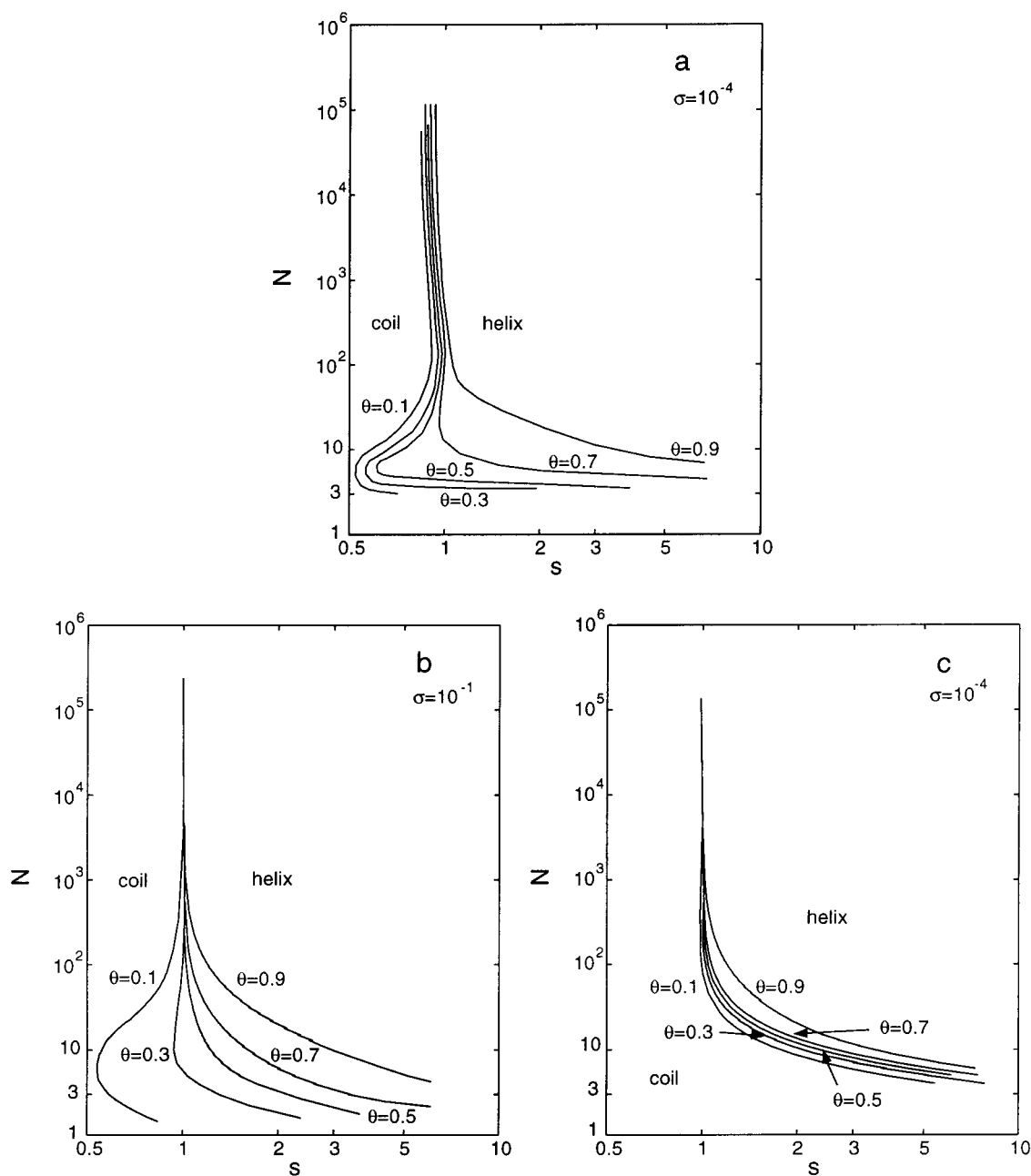


Figure 11. N vs s diagram calculated for (a) our AH model with $\sigma = 10^{-4}$ and for the “zipper” model with (b) $\sigma = 10^{-1}$ and (c) $\sigma = 10^{-4}$. In all the cases, $\theta = 0.1, 0.3, 0.5, 0.7,$ and 0.9 points were searched in the $N - s$ plane with an accuracy of $d\theta = \pm 0.02$. The averages were plotted as solid lines. For the “zipper” model case, we used eqs 20–37 of Cantor and Schimmel v.III to estimate the equilibrium values for θ . A good qualitative agreement with the predictions of the “zipper” model is observed, suggesting that our choice of configurational probabilities leads to realistic equilibrium properties of the AH model.

evidence suggests that the mean sequence approximation underlying our MFP time calculations and the AH model lead to realistic equilibrium properties of the polypeptides.

6. Conclusions

The general features of the *equilibrium* statistical and thermodynamical aspects of the helix–coil transition are largely understood. However, there is great disparity in the variety of current experimental and theoretical estimates of the rate of helix propagation and folding.

In this work, we have presented the AH model that provides a detailed description of the dynamic and equilibrium aspects of the helix–coil transition. Built in the tradition of the classic “Ising” models of ZB and Lifson–Roig, the AH model permits

the evaluation of kinetic aspects of the coil-to-helix transition such as the mean transition time for the formation of any fraction of helix from any initial fraction of coil. This was accomplished through the calculation of mean first-passage times from the backward master equation.

Our study has led to the following conclusions. (1) The use of the “mean sequence” approximation leads to a set of self-consistent equations for the closed form solution of the kinetic and equilibrium properties of the coil-to-helix transition. (2) The “mean sequence” approximation was validated by an analysis of the equilibrium properties that were found to compare well with the classical ZB model. (3) We have generalized the standard mean first-passage time equation to the case of transition rates that depend implicitly on the state of the system.

(4) As an extension of previous theories for the MFP time of transition in Ising-like systems, the solution allows for the examination of the role of cooperativity (interresidue coupling) as well as local bias (intraresidue energetics). (5) By examining the coil-to-helix transition through the solution of the MFP time equation, assumptions regarding (sequential) propagation from single nucleation sites, single coil/helix (zipper) interfaces, and unidirectional (zipper or sequential) helix propagation are avoided. (6) General features of the coil-to-helix transition that have been previously observed, including the dependence of the MFP time on the ZB parameters σ , with inverse scaling as in the theory of Schwartz, and s , where a maximum is seen about s equal to unity as in the work of Gō, are recovered in this work.

In this paper, we used our AH model to estimate the dependence of the rates of helix formation on peptide length. We obtained results consistent with those derived from the sequential model of Brooks. However, our model is built on more detailed estimates of uniresidue transition rates and neighbor-dependent configurational probabilities that describe the kinetic, nonequilibrium aspects of the transition. We include the possibility of multiple nucleation sites and bidirectional propagation of helical segments. As such, our study provides a more detailed understanding of the physical processes that governs the coil-to-helix transition.

Our model provides a framework that can be used to understand the nanosecond time scale helix propagation rates observed in the latest laser temperature-jump experiments for relatively small peptides.^{11,22–24,30} We have shown that relation 2 between the ZB model parameters σ and s and the microscopic interaction energies J and H is an approximation that holds well for relatively small peptides. We also provided a numerical method for estimating the σ and s parameters as functions of J and H which is exact in the frame of our AH model and takes into consideration peptide end effects. Future experiments on homopolymers with the same length, and in the same solvent but with different residue–residue interactions, can test the validity of these relationships. Because our model provides the analytic relationship between mean folding times, helix nucleation, and propagation rates and the most basic parameters that describe the peptide system (J , H , and N), future experiments such as the one suggested above can be easily designed to test it.

A strength of the AH model is that it allows for the calculation of first-passage times between particular states of the model polypeptide over a wide range of energy scales and peptide length scales. We want to emphasize that the general form of the analytic expression for the MFP time, eq 10, permits the estimation of mean folding times for realistic experimental cases in which the initial and final states are not necessary “all coil” or “all helix”. A weakness of the AH model is that it is based on a simplified energetic model of the peptide that is limited, by its nature, in the detail that it can provide regarding the time scale and mechanism for the coil-to-helix transition in polypeptides.

It would be a pleasure to attack the coil-to-helix transition using more sophisticated rate theoretical methods and simulation techniques of the sort that Bruce Berne has been central to the development and application of.³¹ Such methods have provided great insight into the reaction dynamics of molecules in liquids.³² Applications to problems of biomolecular importance have also been made.^{33,34} An example of such a theoretical approach is de Gennes’s effort to extend Kramers theory to the coil-to-helix transition in heteropolymers including polypeptides and DNA.³⁵

Examples of detailed numerical simulations and rate theoretical analysis include studies of ion transport through a membrane channel.^{36,37} However, for large scale conformational transitions involving multiple pathways, such methods appear to be limited.

Alternatively, one might apply an optimization principle derived from a variational rate theory to identify likely transition pathways between fixed reactant (coil) and product (helical) states.^{34,38–41} One such approach, the MaxFlux algorithm,⁴² has been used to isolate variationally optimized reaction pathways for an eleven residue polyalanine peptide.⁴³ A strength of such an approach is that it maintains a detailed, all atom level of description of the peptide energetics. For an all atom peptide model combined with an implicit solvent potential, a variety of pathways were isolated and characterized in terms of the general features of the mechanism for the coil-to-helix transition. It was determined that the helix nucleation can occur at multiple sites; for a significant fraction of the trajectories, the peptide underwent a collapse transition to a compact state from which it would reopen before helix propagation could occur; there was no strong evidence for extended regions of 3_{10} -helical structure observed in reaction intermediates. Such details can only be found when more detailed models than the one presented in this AH model, kinetic master equations,^{16,10} or ingenious automata models⁴⁴ are employed.

An intermediate approach between these simplified models and all atom dynamical calculations rests in the sort of computation pioneered by Czerminski and Elber.⁴⁵ A set of minimum energy configurations are taken as the states of the peptide. Reaction path methods are used to define the energetics of the transition between pairs of connected minima. Transition matrix elements are built using those energetic parameters and a reaction rate model such as transition state theory. The resulting master equation is then solved to explore the peptide’s conformational relaxation dynamics. Such an approach, while computationally intensive, holds the promise of providing detailed kinetic data, of the kind derived from simplified models such as the AH model considered here, for a realistic model of the peptide, its sequence, and solvent energetics.

Given the central importance of the coil-to-helix transition in polypeptides, we can expect a continuing theoretical, computational, and experimental effort devoted to addressing a variety of open questions regarding the role of peptide sequence, length, temperature, pressure, and solvation in determining the time scales and pathways for this fundamental biomolecular process.

Acknowledgment. We are grateful to Alexander M. Bezrzhkovskii and Veaceslav Zalom for helpful comments. The numerical analysis and data visualization were carried out using Fortran 90 and Matlab (The Mathworks, Inc., Natick, MA). J.E.S. gratefully acknowledges the generous support of the National Science Foundation (CHE-9975494), the Petroleum Research Fund of the American Chemical Society (34348-AC6), and the Center for Computational Science at Boston University that provided essential computational resources. J.E.S. would like to acknowledge the great and continuing inspiration and support derived from his association with Bruce Berne. To choose to work for Bruce was one of the few best decisions that he has made in his life.

Appendix: Solving the Mean First-Passage Time Equation

In obtaining a solution for the mean first-passage time eq 8, we use the notation

$$t^+(c) = (N - c)\bar{k}_0(c), \quad \text{and} \quad t^-(c) = c\bar{k}_1(c) \quad (43)$$

where the transition rates depend on the “reaction coordinate”, the helical composition of the polypeptide. We also define as in ref 26

$$\phi(c) = \prod_{z=a+1}^c \frac{t^-(z)}{t^+(z)} \quad (44)$$

and $U(c) = \tau(c + 1) - \tau(c)$ and $S(c) = U(c)/\phi(c)$. Using these definitions, eq 8 can be rewritten

$$t^+(c)U(c) - t^-(c)U(c - 1) = -1 \quad (45)$$

or

$$t^+(c)\phi(c)[S(c) - S(c - 1)] = -1 \quad (46)$$

We take c to be bounded as $a \leq c \leq b$ where the boundary conditions are defined using an absorbing boundary at $c = a$ and a reflective boundary at $c = b$. Therefore, $\tau(a) = 0$, as one is already there, and $\tau(b + 1) = \tau(b)$. We find that

$$S(n) = S(b) + \sum_{m=n+1}^b \frac{1}{t^+(m)\phi(m)} \quad (47)$$

where we use the fact that $S(b) = U(b)/\phi(b) = 0$ as $U(b) = \tau(b + 1) - \tau(b) = 0$. Therefore

$$S(n) = \sum_{m=n+1}^b \frac{1}{t^+(m)\phi(m)} \quad (48)$$

and

$$U(n) = S(n)\phi(n) = \phi(n) \sum_{m=n+1}^b \frac{1}{t^+(m)\phi(m)} \quad (49)$$

On the other hand, if we sum all $U(c)$, we find that

$$\tau(c) = \sum_{n=a}^{c-1} U(n) \quad (50)$$

because $\tau(a) = 0$. Therefore, by using eq 49 in eq 50, the MFP time can be estimated as

$$\tau(c) = \sum_{n=a}^{c-1} \phi(n) \sum_{m=n+1}^b \frac{1}{t^+(m)\phi(m)} \quad (51)$$

In our case, from eqs 43 and 44

$$\frac{1}{\phi(c)} = \binom{N-1}{c} \binom{N-1}{a}^{-1} \prod_{l=1}^c K(l) \quad (52)$$

where $K(l)$ is the ratio of the backward and forward mean transition rates that describe the system in the state l , defined $K(l) = \bar{k}_0(l)/\bar{k}_1(l)$.

Considering eqs 43, 51, and 52, we obtain the mean first-passage time expression

$$\tau(a,b,c,N) = \frac{1}{N} \sum_{n=a}^{c-1} \binom{N-1}{n}^{-1} \sum_{m=n+1}^b \binom{N}{m} \frac{1}{\bar{k}_0(m)} \prod_{l=n+1}^m K(l) \quad (53)$$

Equation 53 is a central result of this paper. It represents the complete analytic expression of the MFP time calculated for a one-dimensional jump process of a system of length N that has an absorbing boundary at $c = a$ and a reflective boundary at $c = b$.

We choose the symbol c for the variable that describes the state of the system because in our specific case, for the helix-coil transition, it represents the number of residues in a coil state. In this case (the coil-to-helix transition), if we choose $a = 0$ and $b = N$ such that $\tau(0) = 0$ and $\tau(N + 1) = \tau(N)$, we obtain

$$\tau(c) = \frac{1}{N} \sum_{n=0}^{c-1} \binom{N-1}{n}^{-1} \sum_{m=n+1}^N \binom{N}{m} \frac{1}{\bar{k}_0(m)} \prod_{l=n+1}^m K(l) \quad (54)$$

It is important to note that besides the configurational parameters that describe the system (a , b , c , and N) the MFP time depends on the energetic parameters of the system (the Hamiltonian) through the transition rates contained in eqs 53 and 54. For the case when K is independent of c , this expression reduces to the result of ZSB.²⁸

References and Notes

- (1) Poland, D.; Scheraga, H. *Theory of Helix-Coil Transitions in Biopolymers*; Academic Press: New York, 1970.
- (2) Cantor, C.; Schimmel, P. *Biophysical chemistry*; W. H. Freeman: San Francisco 1980; Vol. 3.
- (3) Schellman, J. *J. Phys. Chem.* **1958**, *62*, 1485–1494.
- (4) Zimm, B.; Bragg, J. *J. Chem. Phys.* **1959**, *31*, 526–535.
- (5) Lifson, S.; Roig, A. *J. Chem. Phys.* **1963**, *34*.
- (6) Bryngelson, J.; Billings, E. *Physics of Biological Systems: From Molecules to Species*; Springer: New York, 1997; Chapter From Interatomic Interactions to Protein Structure, pp 81–116.
- (7) Scheraga, H. *Pure Appl. Chem.* **1978**, *50*, 315.
- (8) Zana, R. *Biopolymers* **1975**, *14*, 2425–2428.
- (9) Daggett, V.; Levitt, M. *J. Mol. Biol.* **1992**, *223*(4), 1121–1138.
- (10) Brooks, C. *J. Phys. Chem.* **1996**, *100*(7), 2546–2549.
- (11) Thompson, P.; Eaton, W.; Hofrichter, J. *Biochemistry* **1997**, *36*, 9200–9210.
- (12) Klimov, D.; Betancourt, M.; Thirumalai, D. *Fold. Des.* **1998**, *3*(6), 481–496.
- (13) Clarke, D.; Doig, A.; Stapley, B.; Jones, G. *Proc. Natl. Acad. Sci. U.S.A.* **1999**, *96*(13), 7232–7237.
- (14) Schwartz, G. *J. Mol. Biol.* **1965**, *11*, 64–77.
- (15) Craig, M.; Crothers, D. *Biopolymers* **1968**, *6*, 385–399.
- (16) Go, N. *J. Phys. Soc. Jpn.* **1967**, *22*, 416–427.
- (17) Scholtz, J.; Marqusee, S.; Baldwin, R.; York, E.; Stewart, J.; Santoro, M.; Bolen, D. *Proc. Natl. Acad. Sci. U.S.A.* **1991**, *88*(7), 2854–2858.
- (18) Schwartz, G.; Seeling, J. *Biopolymers* **1968**, *6*, 1263–1277.
- (19) Schwartz, G. *Biopolymers* **1968**, *6*, 873–897.
- (20) Weaver, D. *J. Chem. Phys.* **1999**, *110*(12), 6032–6038.
- (21) Jun, B.; Weaver, D. *J. Chem. Phys.* **2000**, *112*(9), 4394–4401.
- (22) Dyer, R.; Gai, F.; Woodruff, W.; Gilmanshin, R.; Callender, R. *Acc. Chem. Res.* **1998**, *31*, 709–716.
- (23) Gilmanshin, R.; Williams, S.; Callender, R.; Woodruff, W.; Dyer, R. *Proc. Natl. Acad. Sci. U.S.A.* **1997**, *94*, 3709–3713.
- (24) Callender, R.; Dyer, R.; Gilmanshin, R.; Woodruff, W. *Annu. Rev. Phys. Chem.* **1998**, *49*, 173–202.
- (25) Weiss, G. *Adv. Chem. Phys.* **1967**, *13*, 1–18.
- (26) Gardiner, C. *Handbook of stochastic methods for physics, chemistry, and the natural sciences*, 2nd ed.; Springer-Verlag: New York, 1985.
- (27) Kampen, N. V. *Stochastic Processes in Physics and Chemistry*; Elsevier Science: New York, 1997.
- (28) Zwanzig, R.; Szabo, A.; Bagghi, B. *Proc. Natl. Acad. Sci. U.S.A.* **1992**, *89*, 20–22.
- (29) Eaton, W.; Munoz, V.; Thompson, P.; Henry, E.; Hofrichter, J. *Acc. Chem. Res.* **1998**, *37*, 745–753.
- (30) Eaton, W.; Munoz, V.; Thompson, P.; Chan, C.; Hofrichter, J. *Curr. Opin. Struct. Biol.* **1997**, *7*, 10–14.
- (31) Berne, B. In *Theoretical and numerical methods in rate theory*; Hanggi, P., Fleming, G., Eds.; World Scientific: London, 1993.
- (32) Berne, B.; Borkovec, M.; Straub, J. *J. Phys. Chem.* **1988**, *92*, 3711–3725.
- (33) Karplus, M. *J. Phys. Chem. B* **2000**, *104*(1), 11–27.

- (34) Straub, J. In *Computational Biochemistry and Biophysics*; Becker, A. D., MacKerell, B. R., Jr., Watanabe, M., Eds.; Marcel Dekker: New York, 2001.
- (35) Gennes, P. D. *J. Stat. Phys.* **1975**, *12*(6), 463–481.
- (36) Roux, R.; Karplus, M. *Annu. Rev. Biophys. Biomol. Struct.* **1994**, *23*, 731–761.
- (37) Elber, R.; Chen, D.; Rojewska, D.; Eisenberg, R. *Biophys. J.* **1995**, *68*(3), 906–924.
- (38) Elber, R. Reaction path studies of biological molecules. In *Recent developments in theoretical studies of proteins*; Elber, R., Ed.; World Scientific: Singapore, 1997; pp 65–136.
- (39) Wolynes, P. In *Complex Systems, SFI Studies in the Sciences of Complexity*; Stein, D. L., Ed.; Addison-Wesley: Longman, MA, 1989; pp 355–387.
- (40) Elber, R.; Meller, J.; Olender, R. *J. Phys. Chem. B* **1999**, *103*, 899–911.
- (41) Olender, R.; Elber, R. *J. Chem. Phys.* **1996**, *105*(20), 9299–9315.
- (42) Huo, S.; Straub, J. *J. Chem. Phys.* **1997**, *107*(13), 5000–5006.
- (43) Huo, S.; Straub, J. *Proteins* **1999**, *36*(2), 249–261.
- (44) Poland, D. *J. Chem. Phys.* **1996**, *105*(3), 1242–1269.
- (45) Czerminski, R.; Elber, R. *J. Chem. Phys.* **1990**, *92*(9), 5580–5601.